Spectrum Sensing Performance of p-norm Detector in Random Network Interference

Vesh Raj Sharma Banjade, Chintha Tellambura, and Hai Jiang
Department of Electrical and Computer Engineering, University of Alberta, Edmonton, AB, Canada
Email: {sharmaba, hai1}@ualberta.ca, chintha@ece.ualberta.ca

Abstract—Spectrum sensing performance of a cognitive radio (CR) deploying the traditional energy detector (ED) degrades in the presence of random network interference where both the number and locations of the interferers are random, thus preventing correct detection of primary user (PU) in the band of interest. However, it is not clear how the ED performance in such random network interference can be improved. Moreover, the previous studies do not consider complete modeling of the wireless environment including the cumulative effects of path-loss, fading and random network interference. We thus take these effects into account and investigate the performance of the p-norm detector, which offers the flexibility of adapting p to the operating conditions (as against fixed $p = 2$ for ED). Such adaptability yields remarkable performance gains over ED (say, 15% gain even at $10\,\text{dB}$ lower (than that for ED) PU signal powers). Further, cooperative spectrum sensing with multiple CRs yields additional performance gains (say, 30% better performance at optimal cooperative detection threshold) compared to single CR based sensing even under the cumulative effects of path-loss, fading and random network interference.

Index Terms—Spectrum sensing, cognitive radio, energy detector, p-norm detector, multipath-fading, shadowing, random network interference.

I. INTRODUCTION

Global mobile data traffic is expected to reach 1.6 zeta-bytes per year by 2018 [1]. Such unprecedented growth will require additional portions of the radio frequency (RF) spectrum for accommodating new wireless users. However, spectrum licensed to primary users (PUs) (say, analog/digital TV) is limited (e.g., about 54-806 MHz), yet remains underutilized across time and space [2]. For example, even three unused TV channels (6-7 MHz per TV channel) occupy more than, say, the scalable bandwidth or the maximum allowable bandwidth for Long-term Evolution (LTE) (20 MHz) or IEEE 802.11af systems, respectively. Such inefficient spectrum utilization hinders the introduction of new wireless users/services. In order to improve spectrum utilization, intelligent devices, called cognitive radios (CRs), may opportunistically communicate over the temporarily unused bands [3]. Such opportunistic communication is possible only if the CRs can effectively detect (sense) a PU channel (spectrum band) to be vacant. However, the accuracy of sensing the available vacant bands depends on wireless channel impairments, noise, as well as interference from other users.

Moreover, the future concept of "networked everything" [4], where every wireless user (device) is virtually connected to every other user, creates massive networks of interconnected devices. This leads to leakage of powers from undesired transmitters in space over relatively large distances thus causing interference to the sensing CR node [5]. Such scenarios may typically arise in heterogeneous network settings, say, while enabling co-existence between IEEE 802.22 Wireless Regional Area Networks (WRANs) and IEEE 802.11af Super Wi-Fi in the TV white spaces where an IEEE 802.11af based small-cell access point (AP) may receive interference from other similar APs or even from the IEEE 802.22 based incumbents [6]. However, 802.22 and 802.11af based systems have different specifications. For example, maximum transmit power for an 802.22 PU is 1000 kW while that for an 802.11af AP is 100 mW [5]. Thus, despite such disparate operating conditions, the CR must make correct decisions on the presence/absence of vacant bands. Moreover, in addition to such disparities, the CR must operate in the presence of a network of interferers where both the number and locations (distances) of the interferers vary randomly. Clearly, such random network interference impairs the spectrum sensing accuracy of the CR.

In such scenarios, the ability of CR nodes to operate without any knowledge of the PU signal structure/parameters is particularly advantageous since these parameters dynamically vary in time and across space depending on the modulation type, radio access technology, operators, and so on. Moreover, estimating those parameters entails additional cost and complexity. Fortunately, the energy detector (ED) operates "blindly" and hence is a popular candidate for spectrum sensing [3]. The ED performance has thus been extensively analyzed in multipath-fading (small-scale fading), shadowing (large-scale fading), multiple antennas, cooperative diversity, and others [3], [7]–[14]. Although these works reveal interesting insights on channel impairments and diversity configurations, the investigation of the impact of random network interference is extremely limited [15]–[17]. While these studies show that random interference from secondary users clearly degrades ED's ability to identify unused spectrum bands, [15]–[17] do not treat the inherent effects of fading (which, henceforth refers to both multipath-fading and shadowing). Moreover, methods to improve the sensing performance against the cumulative effects of multipath-fading, shadowing and random network interference have not yet been reported.

To address these issues, we investigate the CR spectrum sensing performance in path-loss, fading and random network interference. We consider the p-norm detector, which encompasses ED as a special case ($p = 2$) and outperforms it in multipath-fading [18]. However, to the best of our knowledge, the performance of p-norm detector has never been studied in presence of random network interference. In summary, our

contributions are as follows:

(i) As the exact distribution of the p-norm detector decision variable is analytically intractable, we propose a classical central-chi square approximation [19], which leads to conditional (on random variables) detection probability P_d and false alarm probability P_f expressions as functions of path-loss, fading and network parameters.

(ii) Further, the average P_d over fading channels is derived. The derived expression and P_f (from (i)) are then utilized to devise semi-analytical evaluation of the detection performance averaged over the random network model. The devised method saves simulation running-time drastically compared to exhaustive Monte-Carlo iterations performed over all random parameters (noise, fading, interferers). For instance, simulation running-time could be reduced from one day to 125 seconds (details in Section V).

(iii) Finally, the developed framework is extended to cooperative spectrum sensing to explore further possible gains with multiple collaborating CR nodes.

The system model is introduced in Section II. Approximate conditional expressions for P_d and P_f are derived in Section III. Average P_d and P_f expressions over fading and random network interference are presented in Section IV. Novel insights are discussed for single CR based sensing in Section V and for cooperative sensing in Section VI before concluding the paper with Section VII.

II. SYSTEM MODEL

A. Network Model

The network model is shown in Fig. 1. Consider a CR located at the center of a circular disc of radius R so that it can sense the presence/absence of PU transmission within the area $A = \pi R^2$. The PU transmitter is operating at a fixed distance $r_0 \leq R$ from the CR node. Within the same area A, there exist K interferers located at distances $\mathbf{r} = [r_1, r_2, ..., r_K]$ from the sensing CR such that both K and $\mathbf{r}$ vary randomly. Such topological randomness in network interference can be modeled via spatial point processes [20]. While our proposed semi-analytical method is not limited to any particular point process model, we will consider the popular (homogeneous) Poisson point process (PPP) for ease of exposition [20] (Section V). The PPP model is valid when the interferers are randomly distributed over a large area without any correlation between their locations. However, even for correlated locations, the PPP assumption may yield within 1-2 dB accuracy compared to the performance of an actual LTE network [20].

B. Link Model

Denoting the true presence and absence of the PU signal within the CR sensing region by H_1 and H_0, respectively, the n-th received signal sample y_n, $\forall n \in \{1, 2, ..., N\}$, conditioned on K, $\mathbf{r}$ and the PU-CR random fading channel coefficient h, can be expressed as

$$y_n = \begin{cases} w_n + \sum_{k=1}^{K} r_k^{-\alpha/2} s_{k,n} & : H_0, \\ h r_0^{-\alpha/2} s_{P,n} + w_n + \sum_{k=1}^{K} r_k^{-\alpha/2} s_{k,n} & : H_1, \end{cases} \quad (1)$$
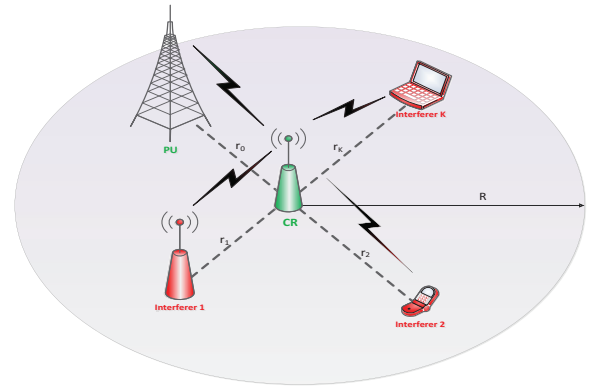
Fig. 1: Network Model. The total number of interferers K and the distances r_k, $\forall k \in \{1, 2, ...K\}$ are random.

where α is the path-loss exponent, $s_{k,n} \sim \mathcal{CN}(0, P_i)$ is the k-th interfering signal sample assumed to be conditionally (on K and $\mathbf{r}$) complex Gaussian with mean zero and variance P_i, $w_n \sim \mathcal{CN}(0, \sigma_w^2)$ is the additive white Gaussian noise (AWGN) sample and $s_{P,n} \sim \mathcal{CN}(0, P_s)$ is complex Gaussian PU signal sample. Note that the statistical modeling of transmit signals as Gaussian is a widely used approach [15]–[17], [21]–[25]. However, deterministic models are also possible [3]. Although our framework may possibly be extended for the deterministic models, they are omitted here for brevity. Also, we disregard the effect of fading on the interfering signals since deep fading of the PU signal (rather than interfering signals) is what determines the sensing performance. In fact, since fading of interfering signals leads to better sensing performance, our assumption of non-faded interfering signals provides a worst-case lower bound on the sensing performance. Without loss of generality, the PU signal, noise and interfering signals are assumed to be mutually independent.

C. The p-norm Detector

The p-norm detector is a generalized version of the traditional ED where the squaring operation is replaced by a power $p > 0$ operation thus yielding a decision variable of the form

$$T = \frac{1}{N} \sum_{n=1}^{N} |y_n|^p, \quad (2)$$

so that the ED ($p = 2$) appears as a special case [25]. The ED is non-optimal in terms of maximizing P_d at fixed P_f, N and signal-to-noise ratio (SNR) or minimizing P_f at fixed P_d and N while the p-norm detector yields a better performance by adapting p to maximize/minimize P_d/P_f, for given values of the other parameters [25]. As well, the ED is non-optimal in detecting signals affected by multipath-fading [18]. These reasons motivate the investigation of the p-norm detector for improving spectrum sensing under cumulative effects of fading and random network interference. We thus derive its P_d and P_f conditioned on the random variables, next.

III. CONDITIONAL DETECTION PERFORMANCE

The detection probability $P_d \triangleq \mathbb{P}(T > \lambda | H_1)$ and the false alarm probability $P_f \triangleq \mathbb{P}(T > \lambda | H_0)$, where λ is the

detection threshold, are two fundamental performance metrics of the p-norm detector. Thus, the statistical distributions of T under H_1 and H_0 are needed to evaluate P_d and P_f, respectively. However, since T is a sum of arbitrary p-th powered random variables, these distributions are not amenable to an exact closed-form analysis even in non-random (non-fading, AWGN) channels [18]. Thus, to date, three distinct approaches for performance analysis of p-norm detector exist, however, with some limitations as follows.

(i) Although highly accurate methods based on the moment-generating function, Laguerre polynomials, and series-sum have been developed for evaluating P_d and P_f [18], the extension of these techniques to the random network and link model at hand appears difficult.

(ii) The central-limit-theorem (CLT) approximation for the distribution of T [26] is only suitable for large samples ($N \gg 1$) and may not facilitate the small-sample performance which is critical to determine the minimum samples (to maintain low sensing time) required for attaining the target sensing performance [24].

(iii) Another approach based on approximating T by a Gamma random variable [25] does not limit the sample size (as in CLT). However, it only considers AWGN channels without encompassing path-loss, fading and/or random network interference.

To circumvent these limitations, we derive approximate P_d and P_f expressions to facilitate analysis of the problem at hand.

We resort to a classical approximation proposed by [19] to approximate the scaled (by ρ) version of T by a central chi-square random variable Y with u degrees of freedom as

$$Y = \frac{1}{\rho} \cdot T. \quad (3)$$

The scaling factor ρ and the degrees of freedom u can be determined by matching the first two exact moments of T/ρ to those of Y. Then, the complementary cumulative distribution functions (CCDFs) of Y under hypotheses H_0 and H_1 yield P_f and P_d, respectively.

For the random signal model considered, the distribution of y_n, $\forall n \in \{1, 2, ..., N\}$, under hypotheses H_0 and H_1, can be expressed as $y_n|H_0 \sim \mathcal{CN}(0, v_0)$ and $y_n|H_1 \sim \mathcal{CN}(0, v_1)$, respectively. The variables v_0 and v_1 denote variances conditioned on the random variables K, $\mathbf{r} = [r_1, r_2, ..., r_K]$ under H_0, and additionally on h under H_1, as

$$v_0 = \sigma_w^2 + \sum_{k=1}^{K} P_i r_k^{-\alpha}$$
$$v_1 = \sigma_w^2 + \sum_{k=1}^{K} P_i r_k^{-\alpha} + |h|^2 P_s r_0^{-\alpha}. \quad (4)$$

Since y_n is conditionally complex Gaussian distributed, its squared amplitude $|y_n|^2$ is exponentially distributed under each hypothesis H_j with the probability density function (PDF) $f_{|y_n|^2}(x) = 1/v_j e^{-x/v_j}$, $j = \{0, 1\}$. Since the samples are independent and identically distributed (i.i.d.), the mean
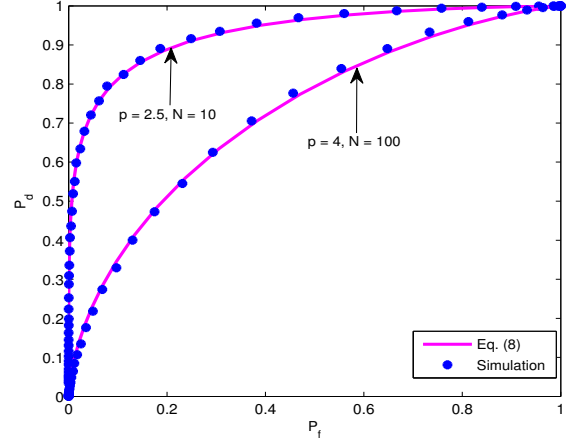
Fig. 2: ROC curves comparing (8) and simulation. The $p = 4$, $N = 100$ graph is plotted for SINR $= -10$ dB and $p = 2.5$, $N = 10$ is obtained with SINR $= 0$ dB.

of $T|H_j$, denoted by μ_j, can be expressed after interchanging the order of integration and summation as

$$\mu_j = \frac{1}{N} \sum_{i=1}^{N} \int_0^\infty x^{p/2} \frac{1}{v_j} e^{-x/v_j} dx = v_j^{p/2} \Gamma\left(\frac{p}{2} + 1\right), \quad (5)$$

where the definition of Gamma function, $\Gamma(a) = \int_0^\infty x^{a-1} e^{-x} dx$, is used. The variance of $T|H_j$, denoted by $var(T|H_j)$, can be obtained similarly as

$$var(T|H_j) = \frac{v_j^p}{N} \left[\Gamma(p+1) - \Gamma^2\left(\frac{p}{2} + 1\right) \right]. \quad (6)$$

Then, using the transformation (3), matching the corresponding means and variances under each H_j, and solving the resulting equations for u and $\rho|H_j$ denoted by ρ_j, $j = \{0, 1\}$, we get (details omitted for brevity)

$$u = \frac{2N\Gamma^2(p/2 + 1)}{\Gamma(p+1) - \Gamma^2(p/2 + 1)}, \quad \rho_j = v_j^{p/2} g(N, p), \quad (7)$$

where $g(N, p) \triangleq [\Gamma(p+1) - \Gamma^2(p/2 + 1)]/[2N\Gamma(p/2 + 1)]$. Then, the CCDFs of Y, for $j = \{0, 1\}$, can be readily derived in terms of the upper-incomplete Gamma function $\Gamma(a, x) = \int_x^\infty t^{a-1} e^{-t} dt$, to yield P_d and P_f, respectively, as

$$P_d \simeq \frac{1}{\Gamma(u/2)} \Gamma\left(\frac{u}{2}, \frac{\lambda}{2\rho_1}\right), \quad P_f \simeq \frac{1}{\Gamma(u/2)} \Gamma\left(\frac{u}{2}, \frac{\lambda}{2\rho_0}\right). \quad (8)$$

These approximate expressions (8) are simple enough to lend analysis in the random network/link model of interest as will be discussed in the next section where we evaluate the average of these metrics over the corresponding random variables.

Before proceeding to the next section, the derived expressions (8) are numerically compared against the simulation results via the receiver operating characteristic (ROC) curves for two p-norm detectors with different sample sizes and conditional (on K, $\mathbf{r}$ and h) signal-to-interference-plus-noise ratios (SINRs), where SINR $\triangleq P_s r_0^{-\alpha} / [\sigma_w^2 + \sum_{k=1}^{K} P_i r_k^{-\alpha}]$ (Fig. 2). For both cases, (8) and simulations match closely, thus validating the accuracy of (8).

IV. Average Detection Performance

As discussed in Section III, P_f is conditioned on the number of interferers K and their distances $\mathbf{r}$ while P_d is additionally conditioned on channel gain h. Thus, complete simulation requires averaging over realizations of the random signals, channel gain, noise and the point process, which results in long running-times, particularly for high interferer densities where the number of interfering nodes can be very large. Thus, simulation-only based evaluations are prohibitively expensive for multiple design perspectives which require inter-relationship among various parameters (such as α, P_s, P_i, p, N and others) across a wide range of values. This motivates us to develop a semi-analytical method for faster computation of average P_f (over K and $\mathbf{r}$), denoted by $\overline{P}_f$, and average P_d, denoted by $\overline{P}_d$ (over K, $\mathbf{r}$ and h), next.

Substituting ρ_1 from (7) into the conditional P_d (8) and integrating over the PDF of the squared amplitude of channel coefficient $|h|^2$, denoted by $f_{|h|^2}(x)$, results into

$$P_{d|\text{PP}} = \frac{1}{\Gamma(u/2)} \int_0^\infty \Gamma\left(\frac{u}{2}, \frac{\lambda/[2g(N,p)]}{(\sigma_a^2 + x P_s r_0^{-\alpha})^{p/2}}\right) f_{|h|^2}(x) dx,$$ (9)

where $\sigma_a^2 \triangleq \sigma_w^2 + \sum_{k=1}^K P_i r_k^{-\alpha}$ and the subscript PP indicates condition on the point process (i.e. on K and $\mathbf{r}$). Since $p > 0$ is a critical parameter of interest, imposing any limitations on its range is unrealistic (for example, assuming p as an integer or confining it to a particular interval, for ease of analysis) for achieving possible gains resulting from fine tuning of p. Unfortunately, this requirement renders the integral in (9) virtually intractable. However, with further algebraic manipulations, the integral can be simplified to obtain $P_{d|\text{PP}}$ as an integral over a finite support of the form

$$P_{d|\text{PP}} = \int_0^{\pi/2} \Gamma\left(\frac{u}{2}, \frac{\lambda/[2g(N,p)]}{(\sigma_a \sec\theta)^p}\right) f_{|h|^2}\left(\frac{\sigma_a^2 \tan^2\theta}{P_s r_0^{-\alpha}}\right) \xi(\theta) d\theta$$ (10)

where $\xi(\theta) \triangleq \frac{2\sigma_a^2 \tan\theta \sec^2\theta}{P_s r_0^{-\alpha}\Gamma(u/2)}$. Note that (10) is a very general expression valid for any multipath-fading, shadowing or diversity combining model with a known PDF $f_{|h|^2}(x)$. Moreover, it can be readily computed in software packages such as MATLAB. Finally, (10) averaged over the point process yields $\overline{P}_d$ as

$$\overline{P}_d = \mathbb{E}_{K,\mathbf{r}}(P_{d|\text{PP}}),$$ (11)

where $\mathbb{E}(\cdot)$ denotes the expectation over the random variables K and $\mathbf{r}$. Thus, (11) only needs to be iteratively averaged over the realizations of the point process while simulations-only based evaluations would require additional iterative simulations over random signals, channel gain h and noise. Note that since P_f (8) is independent of h, its average over the point process, denoted by $\overline{P}_f$, is given by

$$\overline{P}_f = \mathbb{E}_{K,\mathbf{r}}(P_f).$$ (12)

The main advantage of (11) and (12) is a drastic reduction in simulation time compared to the direct (exhaustive) simulations over random signals, h, noise, and the point process. For instance, for a homogeneous PPP with average interferer
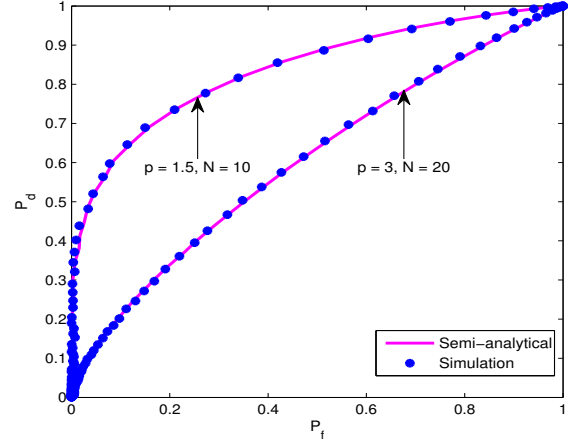
Fig. 3: ROC curves: semi-analytical (11) and (12) vs. simulations for 3-norm, $N = 20$ detector with $\beta = 0.0001$ $\alpha = 4$, $P_i = 10$ dB, $P_s = -10$ dB; and for 1.5-norm $N = 10$ detector with $\beta = 0.005$, $\alpha = 2.5$, $P_i = 5$ dB, $P_s = 0$ dB; $m = 2$, $\sigma_s = 4.66$ dB.

density β over the disc of radius R with the PU-CR link modeled by a Gamma-shadowed Nakagami-m channel (see Section V), in order to attain a 3-digit accuracy for $\beta = 0.0001$ and $\beta = 0.01$ with $R = 150$, the direct simulations require 148 and 1555 seconds, respectively, while our semi-analytical solutions only require 4 and 51 seconds, respectively (on an Intel(R) Core i7(TM), 2.4 GHz CPU). Moreover, say, for $\beta = 0.1$, the average number of interferers is in the order of thousands (7069) and simulations could take more than one day to complete, while our solution only takes 127 seconds.

V. Numerical Setup and Discussions

In this section, we present novel, interesting insights into how the p-norm detector performs under the system model at hand. For numerical purpose, the interfering network is generated via a homogeneous PPP. The PU-CR channel is modeled as a Gamma-shadowed Nakagami-m fading channel. The CR sensing performance is illustrated via ROC curves and the average probability of error, defined as $\overline{P}_e = \mathbb{P}(H_1)(1 - \overline{P}_d) + \mathbb{P}(H_0)P_f$ where $\mathbb{P}(H_j)$, $j = \{0,1\}$ denotes the probability of occurrence of H_j. Without loss of generality, the $\overline{P}_e$ results are obtained assuming equally-likely hypotheses.

For a homogeneous PPP with an average interferer density β, the total number of interferers K is a Poisson distributed random variable with probability mass function $\mathbb{P}(K = k) = (\beta A)^k e^{-\beta A}/k!$, while the distance r_k of the k-th interferer $\forall k \in \{1, 2, ..., K\}$ from the sensing CR is uniformly distributed in the disc of radius R with PDF $f_{r_k}(x) = 2x/R^2$, $0 < x < R$, and $f_{r_k}(x) = 0$, $x \geq R$.

The PDF of the squared envelope $|h|^2$ for the Gamma-shadowed Nakagami-m fading channel is given by [27]

$$f_{|h|^2}(x) = \frac{2b^{\frac{m+m_s}{2}} x^{\frac{m+m_s}{2}-1}}{\Gamma(m)\Gamma(m_s)} \mathcal{K}_{m_s-m}(2\sqrt{bx})$$ (13)

with $b = m_s m/\Omega_s$, where for a shadowing standard deviation σ_s, $m_s = 1/[\exp(\sigma_s^2) - 1]$ represents the inverse shadowing severity, $\Omega_s = \sqrt{(m_s + 1)/m_s}$ is the shadowed area mean
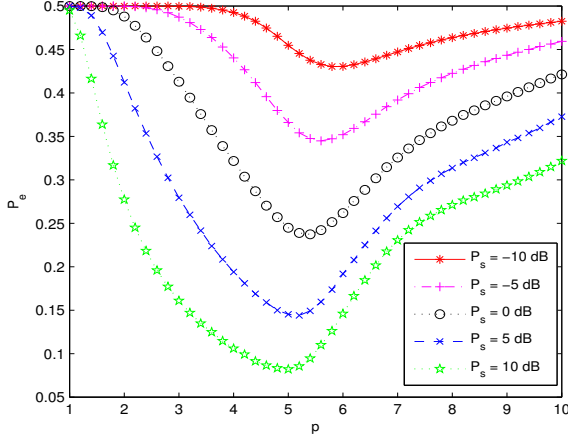
Fig. 4: $\overline{P}_e$ vs. p for various P_s with $N = 20$, $\lambda = 10$, $\beta = 0.0001$, $\alpha = 4$, $P_i = 4\,\mathrm{dB}$, $\sigma_s = 8.686\,\mathrm{dB}$ and $m = 4.5$.
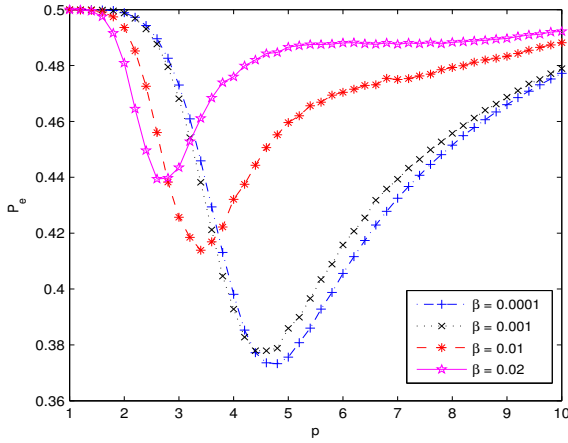
Fig. 5: $\overline{P}_e$ vs. p for various interferer densities β with $N = 10$, $\lambda = 10$ $P_s = 5\,\mathrm{dB}$, $P_i = 5\,\mathrm{dB}$, $\alpha = 2$, $\sigma_s = 6.52\,\mathrm{dB}$ and $m = 2.5$.

power, m is the Nakagami fading severity index, and $\mathcal{K}_\nu(\cdot)$ is the modified Bessel function of second kind of order ν.

Without loss of generality, we normalize the distances with respect to the PU's location $r_0 = 1$ and set $R = 150$. To validate our semi-analytical approach, ROCs obtained using (11) and (12) are numerically compared with those generated from simulations (Fig. 3). A tight match between the two clearly indicates the accuracy of our method.

The dependence of $\overline{P}_e$ on p for various PU signal powers (Fig. 4) clearly indicates that the ED ($p = 2$) is non-optimal in minimizing $\overline{P}_e$ with its performance getting worse for low PU power levels. An optimal p of 5, denoted by $p^* = 5$, attains 71% lower $\overline{P}_e$ than that of ED when $P_s = 10\,\mathrm{dB}$. In fact, another $p^* = 5.4$ detector possesses 15% lower $\overline{P}_e$ than the ED even at $10\,\mathrm{dB}$ lower (than that for the ED) P_s levels.

Another set of graphs (Fig. 5) illustrate the effect of interferer density on the choice of optimal p, which in general, is not equal to 2 (ED). For example with an optimal $p = 4.8$, 25% lower $\overline{P}_e$ (than ED) is attained at $\beta = 0.0001$. More interestingly, the optimal p is inversely proportional to β.

Although the p-norm detector performance in multipath-fading channels is well-characterized [18], its performance
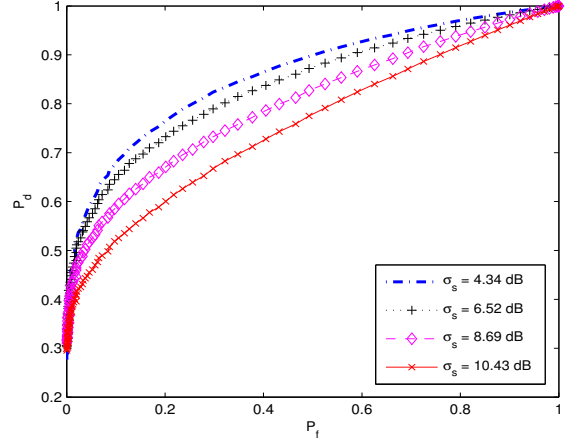
Fig. 6: ROC curves for a 3-norm, $N = 10$ detector for various σ_s dB with $\beta = 0.0001$, $\alpha = 2$, $P_i = 5\,\mathrm{dB}$, $P_s = 0\,\mathrm{dB}$ and $m = 2.5$.

in shadowing is not known. Motivated by this, the effect of shadowing, measured by σ_s dB is explicitly shown in Fig. 6 for a typical outdoor environment (where $4 \leq \sigma_s \,\mathrm{dB} \leq 12$). Clearly, largely shadowed PU signals are more difficult to detect. For example, with a $6.1\,\mathrm{dB}$ increase in the shadowing spread, $\overline{P}_d$ drops by about 23% (at $P_f = 0.01$). A typical solution to mitigate the effects of shadowing is to exploit cooperation among a number of CRs, rather than a single CR detecting the PU, as discussed next.

VI. Cooperative Spectrum Sensing Performance

In cases when the PU is heavily shadowed from the sensing CR, cooperation among multiple CRs remarkably improves the sensing performance [28]. Thus, to mitigate shadowing and more importantly, to explore further enhancements in the sensing performance, we now allow multiple CRs to cooperate.

For cooperatively sensing the PU, multiple CRs participate along with a fusion center (FC) to decide on the presence/absence of PU in the spectrum of interest. Since our primary interest is to evaluate the benefits of cooperation rather than a particular fusion scheme, we do not seek any optimal fusion scheme but simply choose the M out of C fusion rule for the purpose. A discussion of other common fusion rules can be found in [3]. For the M out of C fusion rule, the co-operative (fused) detection probability and false alarm probability, denoted by $\overline{Q}_d$ and $\overline{Q}_f$, respectively, are [29]

$$\overline{Q}_d = \sum_{l=M}^{C} \binom{C}{l} \overline{P}_d^l (1 - \overline{P}_d)^{C-l}; \quad \overline{Q}_f = \sum_{l=M}^{C} \binom{C}{l} \overline{P}_f^l (1 - \overline{P}_f)^{C-l},$$

(14)

where C is the total number of CRs and M is the threshold of cooperative detection such that if the sum of individual 1-bit CR decisions (1 or 0) exceeds (or equals) M, the FC decides in favor of H_1, else it decides on H_0.

Interestingly, cooperative spectrum sensing is advantageous for minimizing the overall probability of error given by $\overline{Q}_e = 1 - \overline{Q}_d + \overline{Q}_f$ (Fig. 7). Say, for $\beta = 0.05$, an optimal M, $M^* = 6$ reduces the probability of error ($\overline{Q}_e$) by 30% as compared to that for single CR ($\overline{P}_e = 0.42$) . Moreover, at
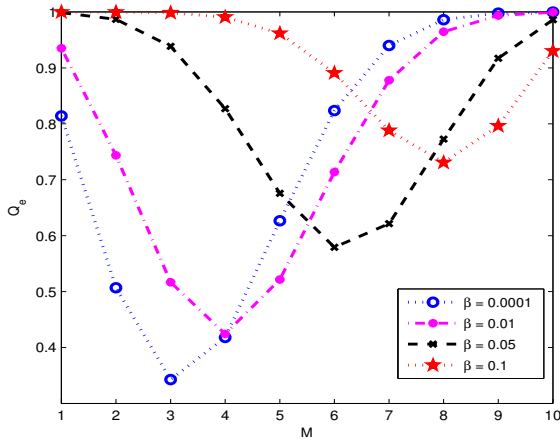
Fig. 7: $\overline{Q}_e$ vs. M with $C = 10$ for various β for a $N = 10$, 4.8-norm detector with $\lambda = 5.5$, $\alpha = 2$, $P_s = -5\,\mathrm{dB}$, $\sigma_s = 8.69\,\mathrm{dB}$, $P_i = 5\,\mathrm{dB}$ and $m = 2.5$.

larger interferer densities, a higher M is better, implying that more CRs deciding in favor of H_1 are needed in order to reduce $\overline{Q}_e$. For example, as much as 27% reduction in $\overline{Q}_e$ can be obtained when M is increased from 1 to 8 for a relatively large interferer density ($\beta = 0.1$).

VII. CONCLUSION

Spectrum sensing with p-norm detector based CR under cumulative effects of path-loss, multipath-/shadow- fading and random network interference has been considered. Adaptive tuning of p in response to varying PU signal power yields better performance, as compared to the traditional ED ($p = 2$) Also, p can be chosen inversely to the interferer density to reduce the impact of random network interference on the sensing performance. Increased levels of shadow-fading degrades the p-norm performance, which however, can be overcome by cooperative spectrum sensing. Additionally, cooperation further improves the sensing performance even in the presence of random network interference. The improvement is achieved by adapting the detection threshold at the FC in proportion to the interferer density. Thus, our technique can serve as a robust tool to design, analyze and improve CR spectrum sensing performance which is fundamental for promoting coexistence among current and next-generation wireless networks.

REFERENCES

[1] Cisco. [Online]. Available: http://www.cisco.com/c/en/us/solutions/collateral/service-provider/ip-ngn-ip-next-generation-network/white_paper_c11-481360.pdf

[2] D. Cabric, S. Mishra, and R. Brodersen, "Implementation issues in spectrum sensing for cognitive radios," in *Proc. Asilomar Conf. Signals, Systems and Computers*, vol. 1, 2004, pp. 772–776.

[3] S. Atapattu, C. Tellambura, and H. Jiang, *Energy Detection for Spectrum Sensing in Cognitive Radio*. Springer, New York, 2014.

[4] Ericsson. [Online]. Available: http://www.akos-rs.si/files/Telekomunikacije/Digitalna_agenda/Internetni_protokol_Ipv6/More-than-50-billion-connected-devices.pdf

[5] C. Ghosh, S. Roy, and D. Cavalcanti, "Coexistence challenges for heterogeneous cognitive wireless networks in TV white spaces," *IEEE Wireless Commun.*, vol. 18, no. 4, pp. 22–31, August 2011.

[6] X. Feng, Q. Zhang, and B. Li, "Enabling co-channel coexistence of 802.22 and 802.11af systems in TV white spaces," in *Proc. IEEE Int. Conf. Commun. (ICC)*, June 2013, pp. 6040–6044.

[7] F. Digham, M.-S. Alouini, and M. K. Simon, "On the energy detection of unknown signals over fading channels," *IEEE Trans. Commun.*, vol. 55, no. 1, pp. 21–24, Jan. 2007.

[8] S. P. Herath, N. Rajatheva, and C. Tellambura, "Energy detection of unknown signals in fading and diversity reception," *IEEE Trans. Commun.*, vol. 59, no. 9, pp. 2443–2453, Sep. 2011.

[9] S. Atapattu, C. Tellambura, and H. Jiang, "Performance of an energy detector over channels with both multipath fading and shadowing," *IEEE Trans. Wireless Commun.*, vol. 9, no. 12, pp. 3662–3670, Dec. 2010.

[10] ——, "Energy detection based cooperative spectrum sensing in cognitive radio networks," *IEEE Trans. Wireless Commun.*, vol. 10, no. 4, pp. 1232–1241, Apr. 2011.

[11] ——, "Analysis of area under the ROC curve of energy detection," *IEEE Trans. Wireless Commun.*, vol. 9, no. 3, pp. 1216–1225, Mar. 2010.

[12] A. Annamalai, O. Olabiyi, S. Alam, O. Odejide, and D. Vaman, "Unified analysis of energy detection of unknown signals over generalized fading channels," in *Proc. IEEE Int. Wireless Commun. and Mobile Computing Conf. (IWCMC)*, July 2011, pp. 636–641.

[13] O. Olabiyi and A. Annamalai, "Further results on the performance of energy detector over generalized fading channels," in *Proc. IEEE Int. Symp. Personal Indoor and Mobile Radio Commun. (PIMRC)*, Sep. 2011, pp. 604–608.

[14] V. Banjade, N. Rajatheva, and C. Tellambura, "Performance analysis of energy detection with multiple correlated antenna cognitive radio in Nakagami-m fading," *IEEE Commun. Lett.*, vol. 16, no. 4, pp. 502–505, Apr. 2012.

[15] A. Makarfi and K. Hamdi, "Efficiency of energy detection for spectrum sensing in a Poisson field of interferers," in *Proc. IEEE Wireless Communications and Networking Conf. (WCNC)*, 2012, pp. 1023–1028.

[16] ——, "Efficiency of energy detection for spectrum sensing in the presence of non-cooperating secondary users," in *Proc. IEEE Global Commun. Conf. (GLOBECOM)*, Dec 2012, pp. 4939–4944.

[17] ——, "Interference analysis of energy detection for spectrum sensing," *IEEE Trans. Veh. Technol.*, vol. 62, no. 6, pp. 2570–2578, July 2013.

[18] V. R. Sharma Banjade, C. Tellambura, and H. Jiang, "Performance of p-norm detector in AWGN, fading, and diversity reception," *IEEE Trans. Veh. Technol.*, vol. 63, no. 7, pp. 3209–3222, Sep. 2014.

[19] P. B. Patnaik, "The non-central χ^2- and F-distributions and their applications," *Biometrika*, vol. 36, no. 1-2, pp. 202–232, 1949.

[20] H. ElSawy, E. Hossain, and D. I. Kim, "HetNets with cognitive small cells: user offloading and distributed channel access techniques," *IEEE Commun. Mag.*, vol. 51, no. 6, pp. 28–36, June 2013.

[21] Y.-C. Liang, Y. Zeng, E. Peh, and A. T. Hoang, "Sensing-throughput tradeoff for cognitive radio networks," *IEEE Trans. Wireless Commun.*, vol. 7, no. 4, pp. 1326–1337, Apr. 2008.

[22] S. Atapattu, C. Tellambura, H. Jiang, and N. Rajatheva, "Unified analysis of low-SNR energy detection and threshold selection," *IEEE Trans. Veh. Technol.*, accepted for publication.

[23] A. Mariani, A. Giorgetti, and M. Chiani, "Effects of noise power estimation on energy detection for cognitive radio applications," *IEEE Trans. Commun.*, vol. 59, no. 12, pp. 3410–3420, Dec. 2011.

[24] L. Rugini, P. Banelli, and G. Leus, "Small sample size performance of the energy detector," *IEEE Commun. Lett.*, vol. 17, no. 9, pp. 1814–1817, Sep. 2013.

[25] Y. Chen, "Improved energy detector for random signals in Gaussian noise," *IEEE Trans. Wireless Commun.*, vol. 9, no. 2, pp. 558–563, Feb. 2010.

[26] F. Moghimi, A. Nasri, , and R. Schober, "Adaptive L_p-norm spectrum sensing for cognitive radio networks," *IEEE Trans. Commun.*, vol. 59, no. 7, pp. 1934–1945, July 2011.

[27] I. Kostic, "Analytical approach to performance analysis for channel subject to shadowing and fading," *IEE Proc. Commun.*, vol. 152, no. 6, pp. 821–827, Dec 2005.

[28] K. Letaief and W. Zhang, "Cooperative communications for cognitive radio networks," *Proc. IEEE*, vol. 97, no. 5, pp. 878–893, May 2009.

[29] W. Zhang, R. Mallik, and K. Letaief, "Optimization of cooperative spectrum sensing with energy detection in cognitive radio networks," *IEEE Trans. Wireless Commun.*, vol. 8, no. 12, pp. 5761–5766, December 2009.